

# Annulated Dialkoxybenzenes as Catholyte Materials for Non-aqueous Redox Flow Batteries: Achieving High Chemical Stability through Bicyclic Substitution

Jingjing Zhang, Zheng Yang, Ilya A. Shkrob, Rajeev S. Assary, Siu on Tung, Benjamin Silcox, Wentao Duan, Junjie Zhang, Chi Cheung Su, Bin Hu, Baofei Pan, Chen Liao, Zhengcheng Zhang, Wei Wang, Larry A. Curtiss, Levi T. Thompson, Xiaoliang Wei,\* and Lu Zhang\*

1,4-Dimethoxybenzene derivatives are materials of choice for use as catholytes in non-aqueous redox flow batteries, as they exhibit high open-circuit potentials and excellent electrochemical reversibility. However, chemical stability of these materials in their oxidized form needs to be improved. Disubstitution in the arene ring is used to suppress parasitic reactions of their radical cations, but this does not fully prevent ring-addition reactions. By incorporating bicyclic substitutions and ether chains into the dialkoxybenzenes, a novel catholyte molecule, 9,10-bis(2-methoxyethoxy)-1,2,3,4,5,6,7,8-octahydro-1,4:5,8-dimethanenoanthracene (BODMA), is obtained and exhibits greater solubility and superior chemical stability in the charged state. A hybrid flow cell containing BODMA is operated for 150 charge–discharge cycles with a minimal loss of capacity.

Redox flow batteries (RFBs) are attractive for large-scale energy storage applications for the electric grid of the future due to their scalable energy capacity and sustained discharge at peak power.<sup>[1–6]</sup> RFBs store charge in energized fluids circulating between the cell and the external tanks. The performance of these devices critically depends on the energy density and chemical stability of the redox active molecules (ROMs) in these fluids. Theoretically, non-aqueous redox flow batteries (NRFBs) can achieve greater energy densities than aqueous systems due to their wider electrochemical windows (>1.5 V).<sup>[7–9]</sup> The focus of this paper is to develop stable ROMs for better performance of NRFBs.

The high-potential ROMs in RFBs are called catholyte molecules.<sup>[10]</sup> Such molecules need to satisfy a number of often orthogonal chemical requirements. In particular, catholyte molecules having the greater redox are more vulnerable to parasitic side reactions as they lack protective groups.<sup>[11,12]</sup> Thus, striking a balance between high energy density and stability has proven to be a difficult task.

1,4-Dimethoxybenzene derivatives (DMBs) have long been considered as leading candidates for use in NRFBs. They have good redox reversibility and high oxidation potentials (4.0–4.8 V vs Li/Li<sup>+</sup>). When bulky alkyl groups are introduced in the 2,5-positions of the arene ring, the chemical stability of oxidized DMBs (i.e., their radical cations) can be improved significantly, as this substitution sterically inhibits ring-addition radical reactions.<sup>[7,9]</sup> Naively, one might expect that further substitution in the arene ring would cause greater stability, yet the opposite occurs; the radical cations become unstable. For instance, 1,4-dimethoxy-2,3,5,6-tetramethyl-benzene (DMTM, **Figure 1**), a fully substituted DMB, is not electrochemically reversible by cyclic voltammetry.<sup>[12]</sup>

In this study, two novel DMB molecules, 9,10-bis(2-methoxyethoxy)-1,2,3,4,5,6,7,8-octahydro-1,4:5,8-dimethanenoanthracene (BODMA) and 9,10-bis(2-methoxyethoxy)-1,2,3,4,5,6,7,8-octahydro-1,4:5,8-diethano-anthracene (BODEA) (see **Figure 1**) have been designed and synthesized as catholyte molecules for NRFBs. The arene rings in these structures are

Dr. J. Zhang, Dr. Z. Yang, Dr. I. A. Shkrob, Dr. R. S. Assary, S. Tung, B. Silcox, Dr. W. Duan, Dr. C. C. Su, Dr. B. Hu, Dr. B. Pan, Dr. C. Liao, Dr. Z. Zhang, Dr. W. Wang, Dr. L. A. Curtiss, Prof. L. T. Thompson, Dr. X. Wei, Dr. L. Zhang

Joint Center for Energy Storage Research  
Argonne National Laboratory

9700 South Cass Avenue, Argonne, IL 60439, USA  
E-mail: xiaoliang.wei@pnnl.gov; luzhang@anl.gov

Dr. J. Zhang, Dr. I. A. Shkrob, Dr. C. C. Su, Dr. B. Hu, Dr. B. Pan, Dr. C. Liao, Dr. Z. Zhang, Dr. L. Zhang  
Chemical Sciences and Engineering Division

Argonne National Laboratory  
9700 South Cass Avenue, Argonne, IL 60439, USA

Dr. Z. Yang, Dr. W. Duan, Dr. W. Wang, Dr. X. Wei  
Energy & Environmental Directorate  
Pacific Northwest National Laboratory  
Richland, WA 99352, USA

Dr. R. S. Assary, Dr. J. Zhang, Dr. L. A. Curtiss  
Materials Science Division  
Argonne National Laboratory  
9700 South Cass Avenue, Argonne, IL 60439, USA

S. Tung, B. Silcox, Prof. L. T. Thompson  
Department of Chemical Engineering  
University of Michigan

2300 Hayward St, Ann Arbor, MI 48109, USA

DOI: 10.1002/aenm.201701272

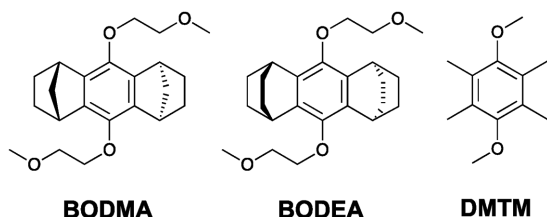


**Figure 1.** Chemical structures of BODMA, BODEA, and DMTM.

fully substituted with similar bicyclic substituents, which are [2:2:1] heptane and [2:2:2] octane like structures for BODMA and BODEA, respectively. These unique substitutions were first introduced by Rathore and Kochi.<sup>[13]</sup> Compared to DMTM, the conformations of these bicyclic substituents are more constrained due to the bicyclic bridging linkages. This enhanced structural rigidity can dramatically impact electrochemical properties, including the electrochemical reversibility.<sup>[13]</sup> As these bicyclic alkyl substituents are hydrophobic (which causes lower solubility of the molecules in polar electrolytes), short ether chains were introduced into 1,4 positions to improve the solubility.<sup>[10,14]</sup> In order to reduce the molecular weight (thereby maximizing the specific charge density), only the shortest ether chains were considered. Further improvements of solubility can be readily attained by further modification of these groups. Details regarding material synthesis and chemical characterization can be found in Section S1 and Figures S1–S4 in the Supporting Information.

**Figure 2** shows the cyclic voltammogram (CV) scans for BODMA and BODEA in 1 M LiTFSI (lithium bis(trifluoromethane)-sulfonimide) in a liquid mixture of ethylene carbonate, propylene carbonate, ethyl methyl carbonate mixed in a weight ratio of 4:1:5 (hereafter referred to as Electrolyte A). **Table 1** summarizes the peak current ratios, redox potentials, diffusion coefficients, conductivity, and solubility of BODMA and BODEA in this electrolyte. CVs exhibit greater reversibility for these two molecules compared to DMTM (see Figure S5 in the Supporting Information). BODMA displayed a reversible redox reaction with the peak current ratio of 1.02 at 4.02 V versus Li/Li<sup>+</sup>. BODEA demonstrated a higher redox potential of 4.18 V versus Li/Li<sup>+</sup> with a lower peak current ratio of 0.26, which indicates inferior reversibility as compared to BODMA. BODMA also has greater solubility and faster diffusion coefficient than BODEA in Electrolyte A.

The improved electrochemical reversibility of BODMA and BODEA with regard to DMTM can be explained by their unique bicyclic substituents. For a typical neutral state DMB, if there were substituents on the arene ring, the alkoxy groups would most likely be out of the plane of the arene ring as the most stable conformation.<sup>[15,16]</sup> However, when the DMB is oxidized to radical cations, the alkoxy groups would rotate into the plane of the arene ring, so that the lone pair electrons on the oxygen atoms can be delocalized with the electrons of the arene ring and an extended conjugation can be achieved, which stabilizes the radical cation and makes it less reactive.<sup>[16]</sup> In DMTM<sup>+</sup>, the methoxy groups are crowded by the adjacent methyl groups in the arene ring; therefore, when oxidized, the conjugation is hampered by the strong steric hindrance, which leads to instability of the radical cation.<sup>[13]</sup> For BODMA

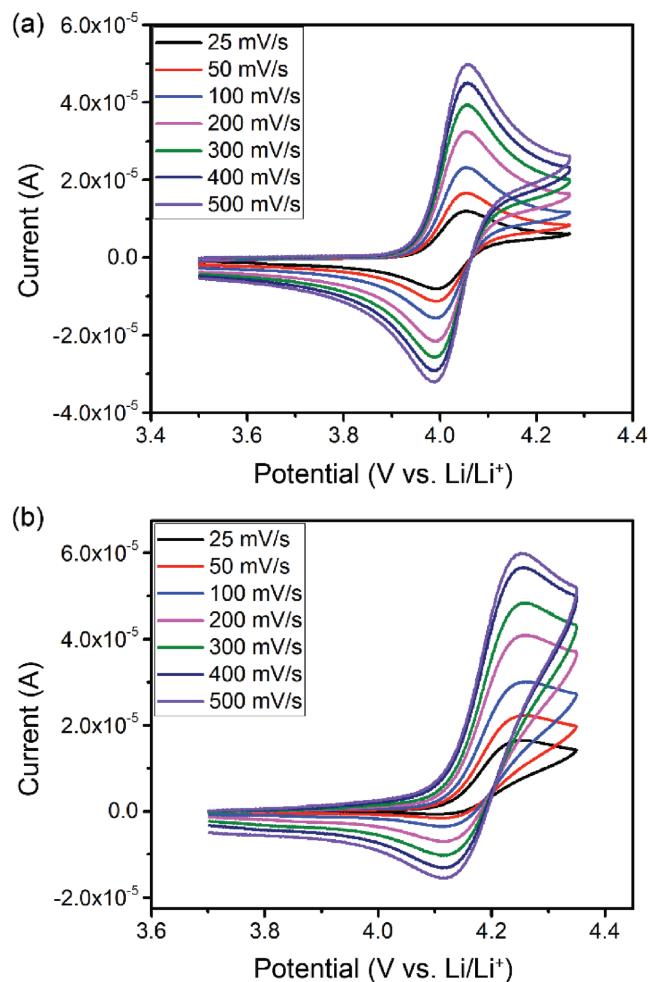


**Figure 2.** Cyclic voltammograms for  $10 \times 10^{-3}$  M a) BODMA and b) BODEA in Electrolyte A obtained using Pt/Li/Li electrodes at 25 °C. The scan rates are given in the plots.

and BODEA, the steric hindrance is reduced significantly due to their constrained conformations. For BODMA, where the bridging linkage is shorter, the spacing between the alkoxy and the [2:2:1] heptane like substituents is greater compared to BODEA. This can be observed in the single crystal structures shown in **Figure 3**. For BODMA (Figure 3a), the bridgehead hydrogen in the bicyclo[2.2.1]heptane group migrates 10° away from the arene plane, and the distance from this hydrogen to the oxygen in the alkoxy group is 2.94 Å; this angle and distance

**Table 1.** Anodic/cathodic peak current ratios, redox potentials, diffusion coefficients, conductivity, and solubility of BODMA and BODEA in Electrolyte A at 25 °C.

Compound	$i_a/i_c$ <sup>a)</sup>	$E_{1/2}$ (vs Li/Li <sup>+</sup> ) <sup>b)</sup> [V]	$\Lambda$ <sup>c)</sup> [mS cm <sup>-1</sup> ]	$D$ <sup>d)</sup> [ $\times 10^{-5}$ cm <sup>2</sup> s <sup>-1</sup> ]	Solubility [mol L <sup>-1</sup> ]
BODMA	1.02	4.02	7.72	4.5	0.15
BODEA	0.26	4.18	8.35	1.1	0.10

<sup>a)</sup>The ratio of anodic/cathodic peak currents; <sup>b)</sup>The average of the cathodic and anodic peak potentials; <sup>c)</sup>Conductivity of 0.1 M solutions at 25 °C; <sup>d)</sup>Diffusion coefficient.

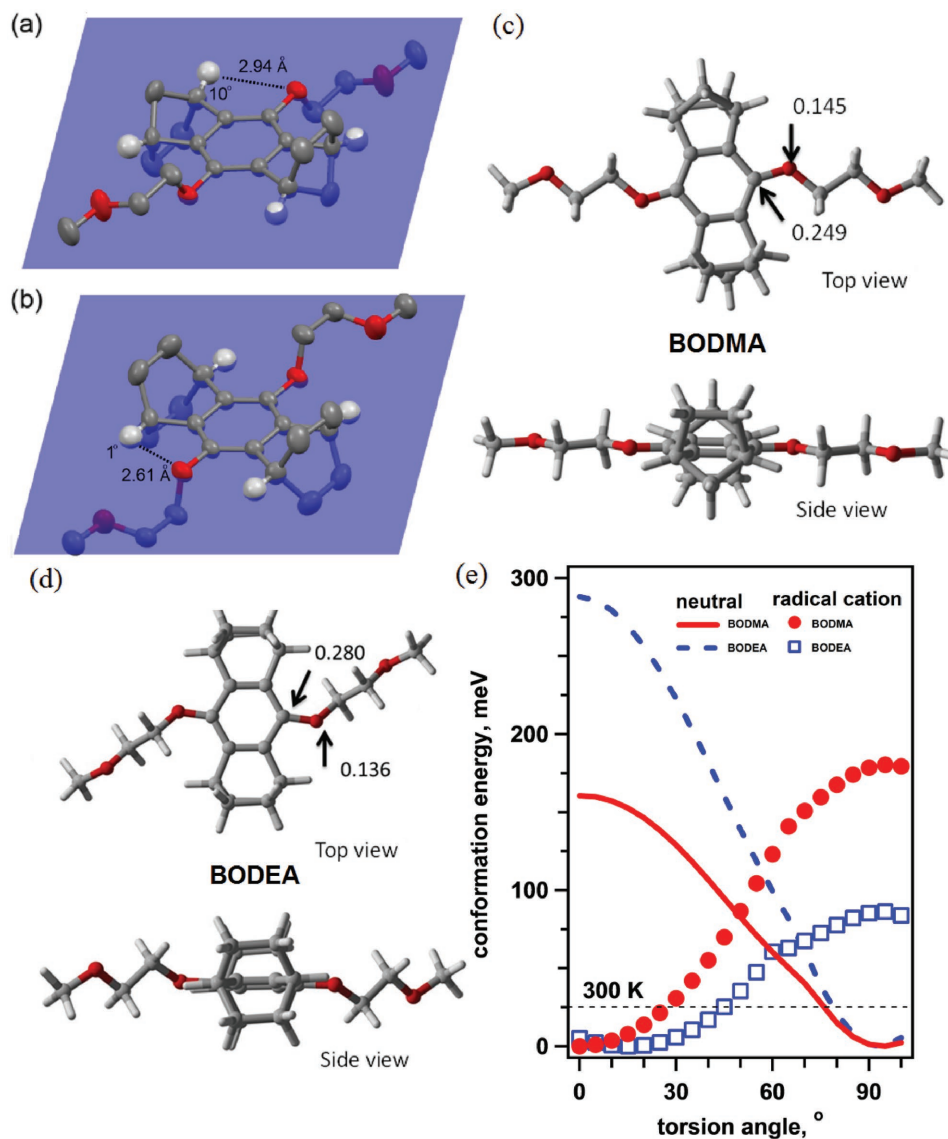


**Figure 3.** a) X-ray crystal structures of BODMA and b) BODEA. Thermal ellipsoids are shown at 50% probability. Some hydrogen atoms are not shown for clarity. The plane of the arene ring is highlighted in blue. c) Optimized structures and selected atomic spin densities of BODMA<sup>•+</sup> and d) BODEA<sup>•+</sup> in the gas phase from the density functional theory calculations. e) Conformational energy for neutral bicyclic substituted molecules (lines) and their radical cations (symbols) plotted versus the torsion angle between the alkoxy (C–O) bond and the plane of the arene ring (with all other degrees of freedom optimized). The dashed line indicates the thermal energy at 300 K (≈25 meV).

can be compared to 1° and 2.61 Å in BODEA (Figure 3b), respectively. Due to the reduced repulsion, BODMA<sup>•+</sup> is more planar (and hence more stable) than BODEA<sup>•+</sup>. A density functional theory calculation was used to examine the conformational changes of the gas phase species in the different states of charge. As shown in Figure S7 (Supporting Information), in the neutral state, the alkoxy groups are perpendicular to the arene plane, whereas in the charged state, these groups rotate near this plane (Figure 3c,d). For BODMA<sup>•+</sup>, the alkoxy groups are almost exactly in the arene plane, whereas for BODEA<sup>•+</sup>, a greater steric hindrance (which is already seen in the neutral state, Figure 3a) causes these groups to rotate ≈16° out of the plane, resulting in less efficient conjugation. The atomic spin densities on the alkoxy oxygen and the adjacent carbon on

arene ring (indicated in Figure 3c,d) are greater in BODMA<sup>•+</sup> as compared to BODEA<sup>•+</sup>, also implying improved conjugation in the former radical cation. Figure 3e shows the plots of the conformational energy versus the torsion angle between the alkoxy groups and the arene ring for BODMA, BODEA, and their radical cations. It is clear from this plot that neutral states are more stable with the 90° torsion angle and radical cations are more stable with the 0° angle. When comparing the two neutral molecules, BODEA has a higher conformational energy at 0° torsion angle, and for the radical cations, a higher conformational energy is also observed for BODEA<sup>•+</sup>, which is consistent with its higher redox potential.

To further assess the stability of these radical cations, electron paramagnetic resonance (EPR) spectroscopy was used

to estimate their hyperfine coupling constants and follow their decay kinetics. The radical cations were generated using bulk electrolysis at a fixed concentration of  $5 \times 10^{-3}$  M in a carbonate electrolyte (Gen2, viz. 1.2 M LiPF<sub>6</sub> in ethylene carbonate/ethyl methyl carbonate in a weight ratio of 3:7). Li/C cell to 100% state of charge. As shown in Figures S8 and S9 in the Supporting Information, both oxidized molecules yield well-resolved EPR spectra. The computationally predicted symmetric structures for radical cations with the alkoxy groups lying near the arene plane are consistent with the observed EPR parameters given in Table S1 (Supporting Information). The kinetics of radical cation decay are also consistent with the anticipated trends. In particular, BODMA<sup>+</sup> showed a longer half-life time of  $\approx 13$  h compared to BODEA<sup>+</sup> (1.4 h). To compare the lifetime of BODMA<sup>+</sup> in different electrolytes, BODMA<sup>+</sup> SbCl<sub>6</sub><sup>-</sup> was synthesized (see Section S1 in the Supporting Information); this paramagnetic salt is stable in a solid form. As shown in Figure S10 in the Supporting Information, the EPR spectra and kinetics of BODMA<sup>+</sup> SbCl<sub>6</sub><sup>-</sup> solutions are similar to the ones obtained for electrochemically generated BODMA<sup>+</sup>. In Figure 4, decay kinetics of BODMA<sup>+</sup> in three polar solvents obtained in this way are compared. The longest half-life time of 120 h was observed in dichloromethane. In a carbonate solvent, the half-life time was reduced to  $\approx 17$  h, and it became still shorter in a more polar acetonitrile solvent (Figure S10, Supporting Information). Unfortunately, while the dichloromethane based electrolytes increase the radical cation stability, they have too low conductivity and excessive volatility to be practically useful in the flow cells.

Given these observations, we reasoned that BODMA in a carbonate electrolyte would make the most suitable catholyte material for NRFBs. Conducive to this application, the solubility of BODMA in Electrolyte A was 0.15 M, and the conductivity of the saturated solution was 7.7 mS cm<sup>-1</sup>. The electrochemical cycling performance was evaluated using a Li/BODMA flow cell with a Li-graphite hybrid anode (Figure 5). The details of

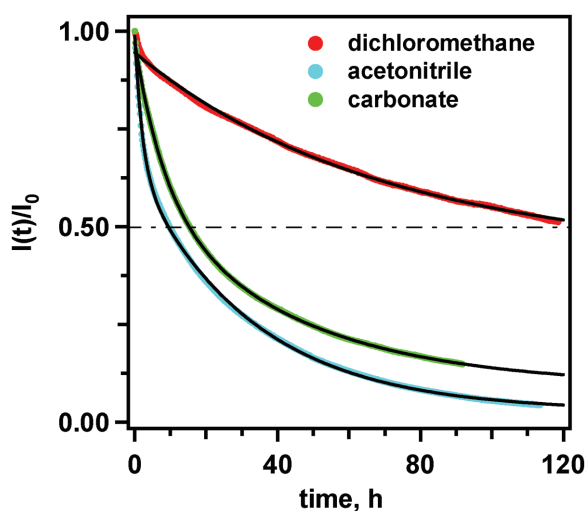


**Figure 4.** Normalized decay kinetics  $I(t)$  of the integrated EPR signal from BODMA<sup>+</sup> in  $5 \times 10^{-3}$  M BODMA<sup>+</sup> SbCl<sub>6</sub><sup>-</sup> solutions in dichloromethane-*d*<sub>2</sub>, acetonitrile-*d*<sub>3</sub>, and a carbonate electrolyte.  $I_0$  is the initial value; the solid black lines are biexponential fit curves.

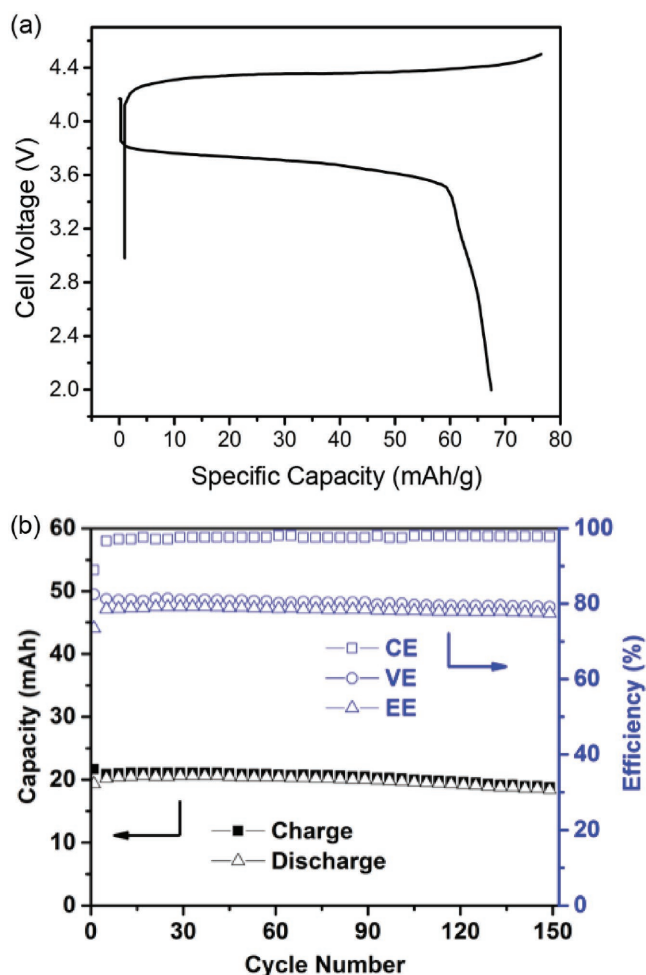


**Figure 5.** a) The representative charge/discharge voltage curve for the Li/BODMA cell. b) Capacity and efficiency profiles of the Li/BODMA cell. The current density was 5 mA cm<sup>-2</sup>.

the setup and the electrochemical tests are given in Section S4 of the Supporting Information. As shown in Figure 5a, in a hybrid flow cell with Li-graphite anode, BODMA delivered a charge plateau at 4.3 V and a discharge voltage of 3.6 V. Compared to the CV results in Figure 1, the difference may originate from the associated overpotential of the flow cell (in which a porous carbon electrode was used instead of a carbon glass electrode). The average charge and discharge specific capacities were 70 and 69 mA h g<sup>-1</sup>, respectively, which represents 94% and 92% of the theoretical capacity, respectively, indicating excellent material utilization ratios. The cell displayed nearly constant cycling efficiencies over 150 charge-discharge cycles with a coulombic efficiency (CE) of 98%, voltage efficiency of 80%, and energy efficiency (EE) of 78% (Figure 5b). The relatively low CE and EE during the first cycle were probably due to formation of a solid-electrolyte interphase on the reactive anode. The capacity of the flow cell was maintained throughout 150 cycles, and the mean capacity retention of 99.97% per cycle was achieved, which indicates excellent chemical and electrochemical stabilities of BODMA (Figure S12 in the Supporting Information shows the effect



of the increased charge rate on these cycling parameters). Although still insufficient for practical grid applications that require years of service, this cycling stability represents a significant progress in redox materials design toward extended cycle life for NRFBs compared to prior analogues of this family and to many other systems.<sup>[7,12]</sup> The exceptional performance of BODMA in these cycling tests places our redox system among the most promising flow cell chemistries reported in the literature to date.<sup>[17]</sup>

In summary, two novel bicyclic substituted dialkoxybenzene molecules, BODMA and BODEA, have been developed for use as catholyte materials in NRFBs. These molecules have been engineered to provide greater solubility (in their neutral state) and improved chemical stability (in their charged state) as compared to other tetra-substituted dialkoxybenzenes. The substitution in the arene ring excludes a large class of parasitic radical reactions resulting in the improved chemical stability. The structural differences between these two bicycloalkyl substituents have considerable effect on their electrochemical behavior and physical properties. Compared to BODEA, BODMA has greater solubility, lower oxidation potential, better electrochemical reversibility, and greater stability of the radical cation in the common carbonate electrolytes. A hybrid flow cell using BODMA as the catholyte material demonstrated stable efficiencies and capacity over 150 cycles. Our study indicates that (when designed properly) full substitution in a small-molecule catholyte material can significantly improve electrochemical cycling performance, widening dramatically the structural space for optimization of such materials for NRFBs.

## Supporting Information

Supporting Information is available from the Wiley Online Library or from the author.

## Acknowledgements

This work was supported as part of the Joint Center for Energy Storage Research (JCESR), an Energy Innovation Hub funded by the U.S. Department of Energy, Office of Science, Basic Energy Sciences.

## Conflict of Interest

The authors declare no conflict of interest.

## Keywords

bicyclic substitution, catholyte materials, non-aqueous redox flow batteries, *para*-dialkoxybenzene

Received: May 9, 2017

Revised: June 6, 2017

Published online: July 21, 2017

- [1] A. Z. Weber, M. M. Mench, J. P. Meyers, P. N. Ross, J. T. Gostick, Q. Liu, *J. Appl. Electrochem.* **2011**, *41*, 1137.
- [2] Y. Yang, G. Zheng, Y. Cui, *Energy Environ. Sci.* **2013**, *6*, 1552.
- [3] G. L. Y. Soloveichik, *Chem. Rev.* **2015**, *115*, 11533.
- [4] K. Gong, Q. Fang, S. Gu, S. F. Y. Li, Y. Yan, *Energy Environ. Sci.* **2015**, *8*, 3515.
- [5] B. Huskinson, M. P. Marshak, C. Suh, S. Er, M. R. Gerhardt, C. J. Galvin, X. Chen, A. Aspuru-Guzik, R. G. Gordon, M. J. Aziz, *Nature.* **2014**, *505*, 195.
- [6] M. L. Perry, A. Z. Weber, *J. Electrochem. Soc.* **2016**, *163*, A5064.
- [7] F. R. Brushett, J. T. Vaughey, A. N. Jansen, *Adv. Energy Mater.* **2012**, *2*, 1390.
- [8] S.-H. Shin, S.-H. Yun, S.-H. Moon, *RSC Adv.* **2013**, *3*, 9095.
- [9] J. A. Kowalski, L. Su, J. D. Milshtein, F. R. Brushett, *Curr. Opin. Chem. Eng.* **2016**, *13*, 45.
- [10] J. Huang, L. Cheng, R. S. Assary, P. Wang, Z. Xue, A. K. Burrell, L. A. Curtiss, L. Zhang, *Adv. Energy Mater.* **2015**, *5*, 1401782.
- [11] J. Huang, I. A. Shkrob, P. Wang, L. Cheng, B. Pan, M. He, C. Liao, Z. Zhang, L. A. Curtiss, L. Zhang, *J. Mater. Chem. A* **2015**, *3*, 7332.
- [12] J. Huang, B. Pan, W. Duan, X. Wei, R. S. Assary, L. Su, F. R. Brushett, L. Cheng, C. Liao, M. S. Ferrandon, W. Wang, Z. Zhang, A. K. Burrell, L. A. Curtiss, I. A. Shkrob, J. S. Moore, L. Zhang, *Sci. Rep.* **2016**, *6*, 32102.
- [13] R. Rathore, J. K. Kochi, *J. Org. Chem.* **1995**, *60*, 4399.
- [14] L. Zhang, Z. Zhang, P. C. Redfern, L. A. Curtiss, K. Amine, *Energy Environ. Sci.* **2012**, *5*, 8204.
- [15] L. Zhang, Z. Zhang, K. Amine, in *Lithium Ion Battery-New Developments*, (Ed: Ilias Belharouak), INTECH, Croatia **2012**, pp. 174–188.
- [16] Z. Chen, Y. Qin, K. Amine, *Electrochim. Acta* **2009**, *54*, 5605.
- [17] Y. Zhao, Y. Ding, J. Song, G. Li, G. Dong, J. B. Goodenough, G. Yu, *Angew. Chem. Int. Ed.* **2014**, *53*, 11036.